IET Microwaves, Antennas & Propagation

An Experimentally Validated Smart Card UHF Tag Antenna For Free Space and Near Body Scenarios

MAP-2019-0603.R2 | Research Article

Submitted on: 09-06-2020

Submitted by: Mahreen Riaz, Mohammad Ghavami, Sandra Dudley

Keywords: RFID ANTENNA, UHF RFID ANTENNAS, UHF MEASUREMENT, BODY WORN, SMART CARDS, METALS

IET Research Journals

Submission Template for IET Research Journal Papers

ISSN 1751-8644
doi: 0000000000
www.ietdl.org

An Experimentally Validated Smart Card UHF Tag Antenna For Free Space And Near Body Scenarios

Mahreen Riaz[1*], *Mohammad Ghavami*[1], *Sandra Dudley*[1]

[1] *Biomedical Engineering and Communications (BiMEC) Research Centre, School of Engineering, London South Bank University, SE10AA, London, U.K.*
[*] *E-mail: riazm4@lsbu.ac.uk*

Abstract:

This investigation primarily promotes a UHF RFID tag antenna for complex environment applications of smart card in free space and near body scenarios. It also considers other high dielectric materials such as water and metallic objects. A dual dipole antenna with T-match structure is chosen due to the advantage of providing high resilience towards change in impedance of high dielectrics, and to ensure the reception of maximum signals at the blind spots of the antenna. The proposed geometry facilitates placement of other off-the-shelf high and low frequency antennas on the card, enabling more features, higher performance, and minimum field interaction between different frequencies. A presented RLC equivalent circuit model estimates the impact of body layers on antenna impedance. A high read range of 7.7 meters in free space, 5.2 meters near body and 2.8 meters at the blind spots is obtained. The novelty is shown by testing the antenna near metals and water, achieving high read range without any design modifications. The proposed tag aims to provide new RFID applications that demand small size, less volume, low cost and multifunctionality over various constraints, while showing good agreement with sensitivity, impedance matching and the read range.

1 Introduction

Radio Frequency Identification (RFID) has seen an enormous egress into our daily lives. It employs RF signals to identify targeted objects and serves in many industrial applications such as medical inventory, laundry management, brand protection, retail inventory, customer service, race timings, security, logistics and asset management [1, 2]. With a cost of $0.10-0.20 for UHF tags mass production, a passive tag's chip does not require an on board battery source and can offer up to 10 meters read range with various dependant factors such as tag use scenario fixed or mobile, directionality, gain, operational frequency and sensitivity, all contribute to the tag's effectiveness [3]. Although RFID technology is robust in free space scenarios, there are some implementation constraints for UHF tags such as proximity issues when the human body, water and metallic objects are present as they exhibit high permittivity values. For instance, if the tag is close to or on the human body, due to high conductivity properties, high power absorption occurs, reducing the gain and ultimately the read range of the tag significantly [4–8]. Conventional mass deployed UHF tag antennas that are designed for free space are mostly unable to display the same performance when used in on-body applications.

In the literature, several tag antennas are presented to overcome these constraints such as [5] where a UHF tag is proposed for perishable goods e.g. meat or milk ensuring a read range of 2.5 to 3 meters in the ETSI band [865.6-867.6 MHz]. In [6], a broadband antenna is presented for near body operations by using two quarter wavelength patch antennas connected with a ground plane on Rogers RT 5880 substrate with dimensions of $67.5 \times 32\ \mathrm{mm}^2$ and $137 \times 32\ \mathrm{mm}^2$, respectively, showing good impedance matching but at the cost of a considerable thickness of 1.575 mm, restricting it to limited space applications. In [9] and [10] a tag is designed on FR4 substrate employed for human body monitoring and metallic cylinder tracking. Considering the line of sight distance, 10 meters read range is achieved in an open space environment and 3.5 to 4 meters is observed for human and metallic object detection, respectively. The reported tag is narrow band and proposed to operate at US frequency band region only. Antennas presented previously have a thickness greater than 0.5 mm [5–8, 11] and some of them use ground planes to reduce the influence of the human body [5] ultimately making them more expensive and difficult to place in smart cards. Another $85.5 \times 54 \times 0.76\ \mathrm{mm}^3$ tag design for a student ID card is presented for on body applications on a PVC substrate for the U.S. frequency band. This tag offers a good read range of 2.7 to 5.7 meters, when placed at various positions on the chest and aligned at the line of sight direction only with the reader antenna at 915 MHz and 4 Watt effective isotropic radiated power (EIRP) thus adding a greater read range than EU EIRP at 3.3 Watt [12]. The large dimensions of the tag does not allow any other antennas to fit in on the card. A single layer wearable dipole UHF tag antenna for human body at 866 MHz is designed with the dimensions of $68 \times 22\ \mathrm{mm}^2$. The gap between the tag and body which affects impedance matching, frequency tuning and realised gain is analysed. The realised gain values are measured in free space and by varying the gap from 4-20 mm. The antenna sensitivity is reduced beyond 8 mm gap. At 4 mm distance the antenna can read up to 3 meters while increasing the distance above 8 mm the theoretical read range of 6-7 meters can be obtained [13]. Another interesting work in [14] shows the effect of on body sewn conductive thread RFID UHF tag and sensor antenna performance. Conductive threads are twisted together with a conductivity of 20 ks/m, significantly lower than pure metals. The sewed tag was attached to the arm of human body and was observed at various angles ranging from 0-360°. Results showed a read range of 1.34 meters at EU frequency band and approximately 4 meters in the air. The potential reason for the lower read range is the employment of the less conductive silver thread as compared to other metals. In [12, 13], the dimensions and thickness of the tags does not permit to fit in limited space of smart cards and the read range of tags at blind spots and other angles is not discussed, thus limiting the scope of applications where line of sight orientation of the tags is not practically possible.

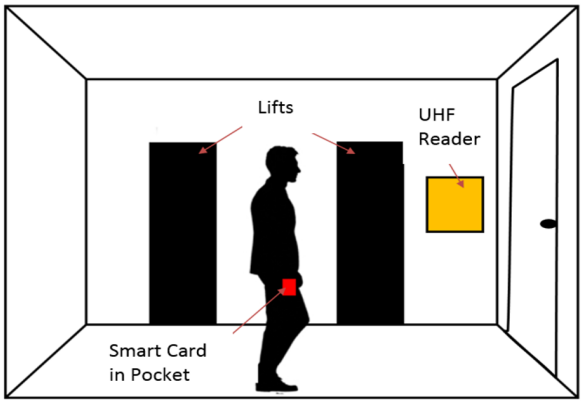

Fig. 1: Scenario of smart card near body.

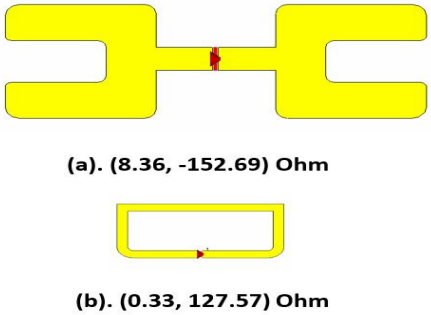

Fig. 2: UHF antenna without inductive loop.

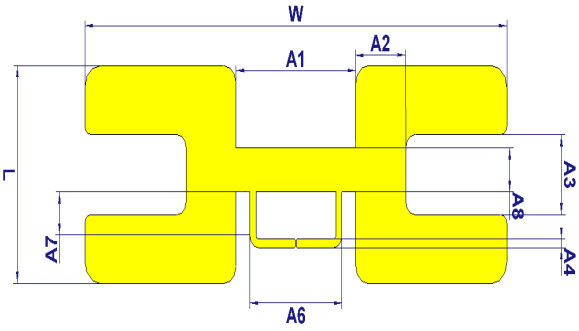

Fig. 3: Dimensions of the proposed UHF antenna.

The performance of the UHF tag is severely affected near a metallic surface. There are several RFID antenna structures proposed for metallic object tagging. Metals are electromagnetic reflectors and radio signals are unable to penetrate them. Several solutions are proposed such as; a foam sheet of at least 3 mm thickness between metallic surface and antenna, using metamaterials or printed inverted-F antennas (PIFA). In [15], two UHF microstrip dipole antennas are proposed to operate at 919 - 923 MHz with the dimensions of $58 \times 34 \times 0.8$ mm^3 comprising three layers, copper traces, a Roger 5880 substrate and a full copper ground plane. The read range obtained from both tag antennas is 2 and 2.2 meters, respectively. Although these tags are good candidates for metallic surface tagging with even considerable thickness and dimensions they are not suitable for limited area applications and read range does not ensure long range detection. Another proposed approach to apply tags on metallic objects is to use commercial RFID tags and attaching a 2.5 mm thick sheet of Styrofoam 103.7 on the back side of tag to avoid any interference with magnetic field. The Styrofoam sheet assist in radiating electromagnetic field on the top side of RFID tag. This method achieves a read range of 2 meters in a straight line and comparable to off shelf expensive tags used for the metallic mounting [16].
UHF tags are also sensitive to the presence of liquids as they increase the resistance loss in the equivalent circuit of the subject antenna. The likelihood of signals being absorbed in liquids is greater at higher frequency band. Several solutions are proposed similar to those at near body and metallic surfaces, such as ground plane to tolerate the effect of liquid or embedding tag inside the cork. These solutions are costly and bulky as compared to label type tags. To overcome these challenges, an off-shelf ALN-9768 Wonder Dog tag is chosen from Alien. Based on the study of equivalent circuit modelling to consider the effect of water, a modified tag is proposed by adding a small resistance in parallel to the actual resistance of the antenna. The proposed tag bandwidth is increased from 3.7 % to 13.5 % of -10 dB. The achieved read range is increased from 1.5 to 2.2 meters in free space and from 0.22 to 0.31 meters in line of sight measurement for glass bottle filled with the liquid. Although the read range is improved but still it is not a good candidate for long range detection [17]. Thus, UHF tags can be customised for use near metals and other high dielectric materials such as liquid bottles but the design geometry needs to be optimised accordingly and based on published research, the tag width should be thick enough to reduce the effect of interference caused by strong magnetic field. Most of the research papers have shown the line of sight measurements and there is limited or no information of read range at the blind spots of the antennas thus limiting the wide applications of tags.
Based on above mentioned challenges, it is very important for the UHF passive tag industry to design antennas that are low in cost, small in size, provide competitive read range at the blind spots of the antenna and compatible with other high dielectric materials. The scope of this paper focuses on free space and near body applications. It also highlights the impact of other high dielectric materials on the performance of antenna, such as water and metallic objects.
There are various UHF dipole antennas proposed in the literature, but most of them are good in terms of providing long read range in line-of-sight for free space scenarios, but in our consideration, a broadband UHF RFID tag antenna is proposed covering the 860-960 MHz frequency region for high dielectric materials such as near body, water and metallic objects. The suggested shape that meets the performance criteria near high dielectrics is dual dipole antenna geometry with a T-match structure. This geometry offers reception of more signals at the blind spots. Also, the half wavelength structure of dual dipole geometry is observed as highly resilient towards change in resistance and reactance values. The high resilience with good conjugate impedance matching with the chip and high gain, contributes towards good read range for free space while ensuring a competitive range for high dielectric materials. Another target is to overcome the issues of few or no detections at the blind spots of antenna, which is met by optimising the geometry parameters to obtain wide blind spots. The read range of the tag ensures detection at difficult to read angles, aiding end users to maintain the required minimum and maximum distance between the reader and the tag at installation sites. The hall installed system successfully detects people and it can be used at various locations such as conference rooms, universities, entrance points of shopping centres or in corridors as shown in Fig. 1.

2 Antenna Design Consideration

The proposed length of the UHF tag is calculated using $L = 0.5 \times c/f$, but the unmodified conventional half-wave dipole antenna is not significant as the reactance is too small to offer conjugate matching with typical RFID IC, and also the size is very large to fit in

Table 1 UHF tag dimension parameters.

Parameters	Dimensions (mm)
L	25.14
W	69.80
A1	19.80
A2	8.27
A3	9.26
A4	1
A5	2.28
A6	15.24
A7	4.96

most of the RFID applications. Therefore, some modifications are required to achieve high performance. In literature, the dual dipole shapes are also suggested for card size applications. The proposed geometry of the tag antenna is a half-wave dual-dipole [18] with an overall dimension of $25.14 \times 69.80 \times 0.05\ \mathrm{mm}^3$ as shown in Fig. 3 and Table 1.

The simulation of the dual dipole structure, which is approximately half-wavelength, contributing to the real impedance as shown in Fig. 2 (a) without any matching structure to show that the antenna is highly capacitive with impedance of Z_{ant}= 8.36 - j152.69 Ω which needs to have a modification to make it inductive. The closed loop of the antenna is based on a T-Match structure to meet the high inductance requirements to achieve conjugate matching with the capacitive impedance of the chip as shown in Fig. 2 (b) with Z_{ant}= 0.33 + j127.57 Ω impedance. Moreover, this dual dipole structure has an advantage over conventional dipole antennas by offering high resilience towards change in impedance values near high dielectric materials. As can be seen in Fig. 3, this design has a large metal surface to offer better performance for placement against high dielectric surfaces, such as in proximity of human body or other high dielectric materials.

A curved shape is applied to reduce the effect of diffracted fields from the antenna edges. These edges ensure reception of more signal rays from the transmitting antenna, which provide sufficient amplitude signals and increase antenna directivity [19]. The overall antenna impedance comprises a T-match short circuited stub and the dual-dipole structure. The closed loop has a length A6 ≤ W, is connected to the dual dipole at the length A7 from the main structure as shown in Fig. 3. The overall impedance at source point is given as [20]:

$$Z_{\mathrm{ant}} = \frac{2Z_t(1+\alpha)^2 Z_a}{2Z_t + (1+\alpha)^2 Z_a} \tag{1}$$

whereas, $Z_t = jZ_0 \tan kA6/2$ is the input impedance of the short circuit stub. Moreover, $Z_0 = 276 \log_{10} b/\sqrt{r_e r_e'}$ is the characteristics impedance of the two conductors with a spacing of A7 between them. Z_a is the antenna impedance value taken without the T-match short circuit stub. The term $r_e = 0.25 \times A4$ and $r_e' = 8.25 \times A8$ are the radii of the dual dipole and matching stub, respectively. While, α can be defined as the current division factor between T-match and dual dipoles of the antenna [20]:

$$\alpha = \frac{\ln(A7/r_e')}{\ln(A7/r_e)} \tag{2}$$

In passive UHF antennas, the tag is designed based on the complex impedance matching with the associated RFID chip [21]. The proposed tag is simulated via CST considering a Monza R6 chip with

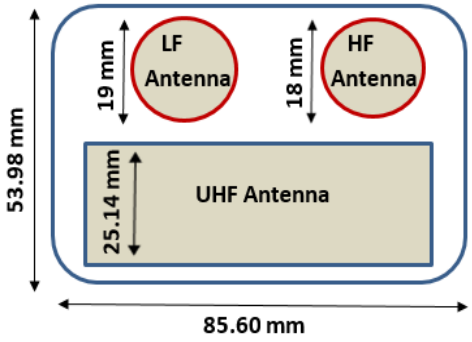

Fig. 4: Triple Tech card space allocation with LF, HF and UHF antenna placement.

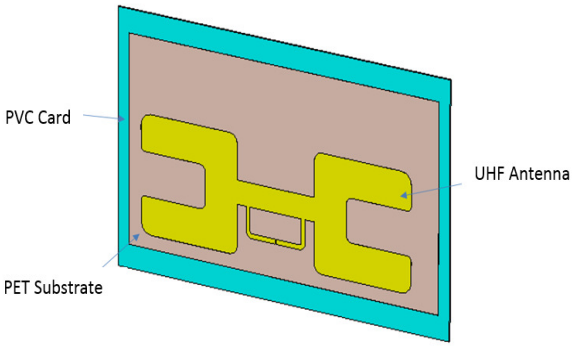

Fig. 5: Schematic of UHF antenna enclosed in the PVC card.

a capacitive impedance of Z_{chip}= 13.5 - j126.56 Ω at 866 MHz and demands a highly inductive antenna to achieve appropriate conjugate matching at Z_{ant}= 13.5 + j126.56 Ω. All the structural dimensions are considered by simulating the antenna into CST software and focusing on achieving another important factor of wide blind spot radiation pattern by considering gap A3. The gap is directly proportional to the gain values of antenna. Whereas, the height of loading bar A8 on A3 on top of inductive loop results in increasing gain values. The parameters A6, A7 and A4 of the loop are adjusted to match the complex chip impedance. The overall antenna geometry is designed to achieve half wavelength at frequency of 866 MHz. In the simulation by introducing the T-match combined dual-dipole structure the overall length is reduced by 60.34% of the antenna wavelength increasing its potential for smart card applications. This tag is designed to fit within a smart Triple Tech card as shown in Fig. 4 along with an LF antenna operating at 125 kHz and a HF antenna with an operating frequency of 13.56 MHz. The dimension of the Triple Tech card is $85.60 \times 53.98\ \mathrm{mm}^2$. The diameters of LF and HF antennas are 19 mm and 18 mm, respectively. The antenna sizes are chosen carefully to ensure appropriate placement into the limited space of the card, with a maximum gap ensured among antennas to avoid any interference.

This research work focuses on the UHF antenna design, simulation and realized antenna performance comparison. Two primary scenarios are considered for modelling and experimental validation of the proposed UHF tag antenna. The first scenario is in free space when a person is holding a card in the lanyard, away from the body. The second scenario covers near body simulations such as when the person has placed the card in a wallet and that wallet is in the pocket.

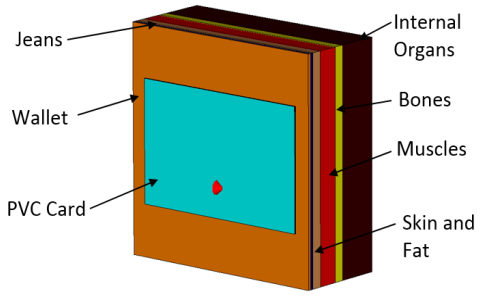

Fig. 6: UHF tag enclosed in a PVC card on human body patch.

Table 2 UHF tag dimension parameters.

Layers	Thickness (mm)	Relative permittivity k (ϵ_r)	Electrical conductivity σ (S/m)
Internal Organs	20	52.1	0.91
Bones	5	20.8	0.33
Muscles	10	55.1	0.93
Skin and Fat	5	14.5	0.25
Jeans	1.5	2.1	0.002
Leather	1.5	1.7	0.001

2.1 *Tag Antenna in Free Space Scenario*

This section covers the first scenario, when UHF antenna is positioned at the bottom of a card and placed in the lanyard or in free space, the proposed design is simulated in the CST software by enclosing the UHF tag on a Polyethylene terephthalate (PET) substrate in the PVC card as shown in Fig. 5. The overall thickness of the PVC card is 0.72 mm, half below and half above the UHF tag, the UHF antenna has 0.01 mm thickness and is made up of aluminum and the PET substrate has 0.05 mm thickness with ϵ_r = 3 enclosed in the PVC card.

2.2 *Tag Antenna in Near Body Scenario*

A scenario is considered to demonstrate a person holding the smart card enclosed with the UHF antenna near the body as shown in Fig. 1. In daily life, this situation is realised when a person typically holds the card in the wallet and places in the pocket. The scenario is modelled in CST as shown in Fig. 6 by creating 100×100 mm^2 patch of human body with layers beginning from the internal organs, bones, muscles, skin and fat, jeans to replicate the pocket, leather for the wallet and the PVC card by using parameters mentioned in Table 2 [22, 23].

3 SIMULATIONS RESULTS ANALYSIS

The effect of a human body on the radiation pattern, gain and input impedance variation are investigated in this section. The directivity of the proposed antenna in free space is 2.1 dBi with a radiation efficiency of 70% and gain of 0.5437 dB. For near body scenario, it behaves more like a directive antenna due to the presence of the highly dielectric body by increasing its directivity to 5.853 dBi and low radiation efficiency of 2.15% which consequently reduces the

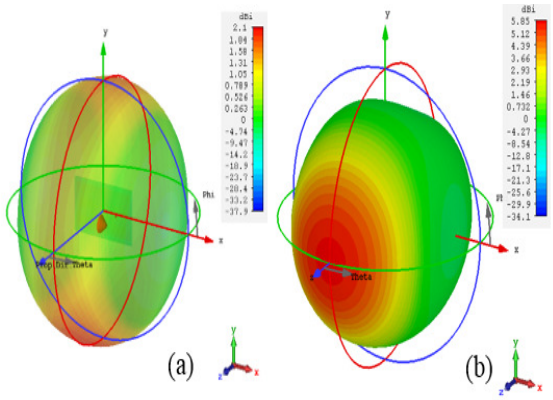

Fig. 7: Radiation pattern of UHF tag in (a) Free space and (b) Near body scenario.

gain of the antenna from 0.5437 dB to -10.82 dB as shown in Fig. 7. Various simulations are performed to investigate the impact of each layer on the proposed UHF antenna design as shown in Fig. 8. It can be seen that the UHF antenna's real impedance varies from 0.776 Ω for the free space scenario to 34.25 Ω for a near body scenario, whilst for the imaginary part, the variance is from 122.66 Ω to 125.37 Ω. Body layers offer high permittivity and conductivity which is inversely proportional to resistivity and offers low resistance for individual layers as shown in (3). Each layer of the body behaves as a high pass filter and is explained in more details in section 4. Resistance adds in a reciprocal fashion, therefore lower values show high impact on the real impedance graph when summed together. On the other hand, parallel capacitance adds in series and produces less effect on the imaginary impedance.The impedance displays excellent resilience towards trivial changes in the antenna reactance, the imaginary part shows a very small overall change of -3% and -0.94% for open air and near body scenarios, respectively while for the real part there is a considerable change. The results show a good conjugate impedance match of the antenna with the RFID chip as shown in columns (a) and (c) of Table 3.

4 EQUIVALENT CIRCUITS OF FREE SPACE AND NEAR BODY SCENARIOS

This section presents the equivalent RLC circuit modelling of the tag for free space and near body scenarios. It explains a simple and efficient way to approximate antenna behaviour by circuit modelling and considering the layers of a human body interacting with the UHF antenna and chip. Modelling of the free space scenario shows two main structures comprising the RFID chip and UHF antenna.While, the near body scenario modelling consists of three main structures UHF tag antenna, the RFID chip and a human body model. Various investigations have shown human body model structural simulations [24] but there are no publications, to the best of our knowledge, to describe basic RLC circuitry modelling representing the human body structure layers with an antenna and chip to aid understanding of the effects of each component on the overall antenna performance. The human body contains a large number of water molecules which absorb RF radiation energy and act as capacitors in the RFID environment causing signal absorption, ultimately resulting in degradation of tag detection. The electrical properties of the human body such as permittivity and conductivity vary from person to person and depend upon skin thickness, area of the body under consideration and ethnicity [25]. A comparison of RLC equivalent circuits with 3D modelling and realised results is provided in Table 3 and section 5, demonstrating the accuracy of the proposed model.

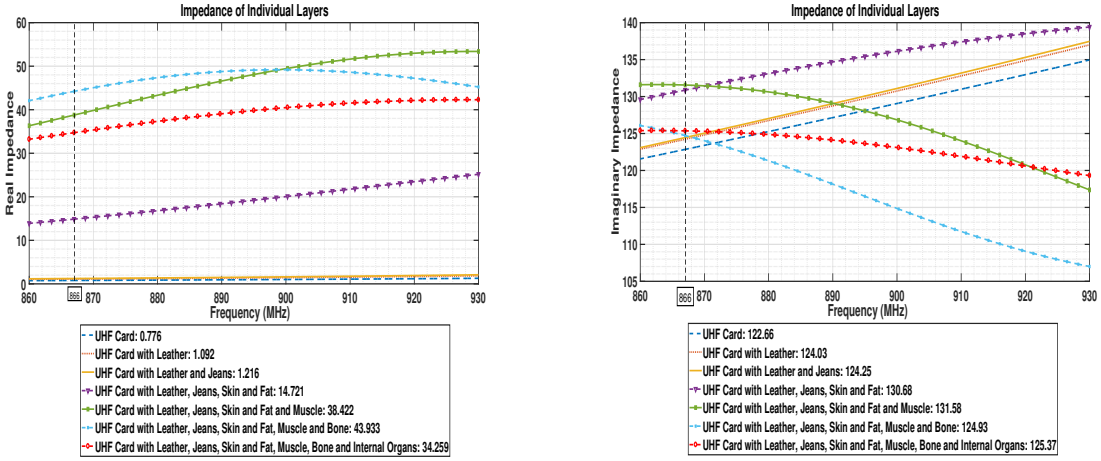

Fig. 8: Impedance variation in ohms by adding layers of the proposed model. (a) Real impedance (b) Imaginary impedance

Table 3 Impedance values in ohms under different scenarios at 866 MHz.

Scenario	Smart card 3D simulation	Smart card circuit modelling	Smart card near body 3D simulation	Smart card with the body [28] RLC modelling	Smart card by the proposed RLC modelling
	Column (a) Fig 4	Column (b) Fig 9	Column (c) Fig 5	Column (d) Fig 10	Column (e) Fig 11
Without RFID Chip	0.77 + j122.6	0.7 + j122.64	34.25 + j125.37	-	25.44 + j122.6
With RFID Chip	14.27 - j 4.95	14.19 - j3.55	47.55 - j1.63	31.55 +j2.92	38.93 - j3.61

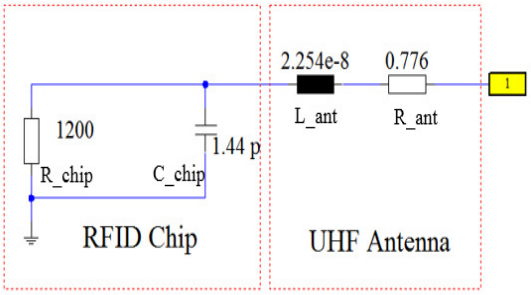

Fig. 9: Equivalent circuit model of UHF RFID antenna and the chip.

4.1 Equivalent Circuit Model of UHF Tag in Free Space Scenario

The UHF antenna and Monza R6 chip model which is a representation of Passive Band Pass Filter for free space scenario is shown in Fig. 9. The resistance and inductance values of UHF antenna enclosed in the PVC card are taken from the circuit simulations performed in the CST Design Studio and RFID chip values are taken from Monza R6 manual. The equivalent RF model of the chip and antenna is simulated as shown in [26, 27].The circuit modelling results of an antenna with and without chip are shown in column (b) of Table 3, it can be observed that at the resonance point in RLC circuit, the capacitance of the chip is cancelled by the highly inductive reactance of the antenna by providing only real resistance values.

4.2 Equivalent Circuit Model of UHF Tag in Near Body Scenario

In [28], human body impedance analysis was performed to estimate the electrical properties of tissues. The equivalent circuit model consists of five high-pass filters (HPF) to represent the human body impedance from the path of right to left hands and accommodating changes with frequency. The electrical model consists of resistance R of the liquid inside and outside of the cell in parallel with the capacitance C showing the conductance of cell membrane at high frequencies. The suggested model is simulated with the UHF antenna and RFID chip to see the overall impact of human body in terms of impedance as shown in Fig. 10. The antenna and chip RLC model is taken from Fig. 9, the free space scenario and combined serially with the suggested model. The equivalent model at the

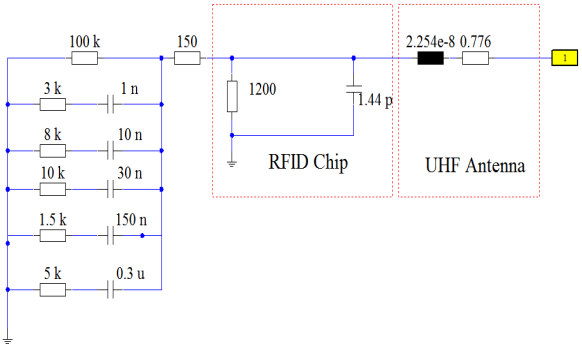

Fig. 10: Equivalent circuit model of the human body with UHF RFID antenna and the chip.

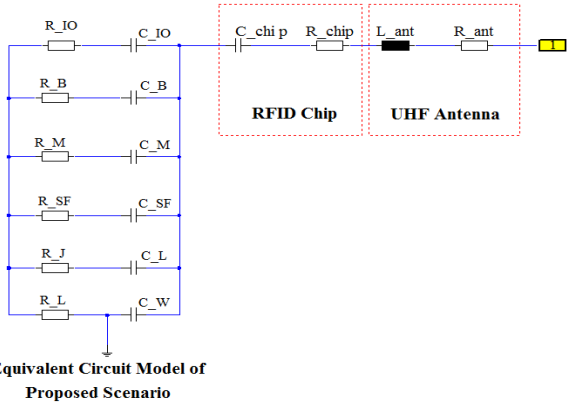

Fig. 11: Proposed equivalent circuit model of human body with UHF RFID antenna and the chip.

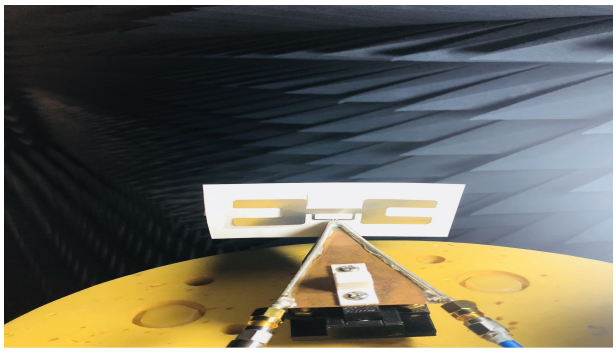

Fig. 12: UHF tag testing in anechoic chamber by using balun.

866 MHz resonant frequency shows conjugate matching of the RFID chip and antenna by leaving the impact of pure resistance and human body impedance on the combined structure as shown in column (d) of Table 3. It can be observed that the real and imaginary impedance values with the chip are dissimulating from 3D simulation results of the near body scenario. The major reasons could be the consideration of different body area as it from left to right hands and also it does not consider the equivalent structure of jeans and leather layers in the RLC model.

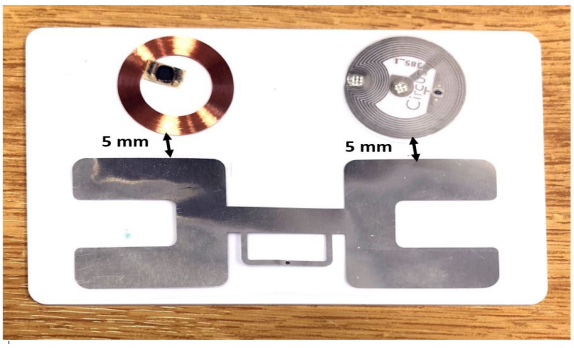

Fig. 13: Realised smart card with UHF, LF and HF tags.

Table 4 RLC circuit values for proposed human body layers.

Layers	Resistance (R)	Value (Ω)	Capacitance (C)	Value (ρF)
Internal Organs	R_{IO}	54.9	C_{IO}	923
Bones	R_B	606	C_B	1470
Muscles	R_M	107.5	C_M	1950
Skin and Fat	R_{SF}	88.8	C_{SF}	1027
Jeans	R_J	293 K	C_J	495
Leather	R_L	553.1K	C_L	100

4.3 The Proposed Equivalent Circuit Model of the UHF Tag in Near Body Scenario

In this section, an RLC circuitry is proposed as shown in Fig. 11 by using 6 HPFs for individual layers that are represented in Fig. 6 to calculate the impedance and to represent the approximate equivalent 3D structure of the human body presented in [23] along with jeans and leather layers as shown in Table 2 together with the UHF tag and the chip. A comparison is performed between [28] and proposed equivalent structure to analyse the difference in considering different body structures and validating proposed method. The resistance and capacitance of the layers are calculated using (3):

$$C = \frac{k\varepsilon_0 A}{d}, \quad R = \frac{\rho L}{A}, \quad \sigma = \frac{1}{\rho} \tag{3}$$

whereas, C represents the capacitance of the body layers, k is the relative permittivity of the material, ϵ_0 is the permittivity of free space 8.854×10^{-12} F/m, A represents the surface area of the plates which is human body layers in our case and d is the distance between two consecutive layers. In case of resistance R, ρ is the electrical resistivity, A represents the cross-sectional area and L shows the length of the material under observation. Moreover, the inverse of the electrical resistivity is the conductivity σ. For simplicity, the RFID chip model is converted from parallel to series equivalent. The circuitry values are shown in Table 4. The results of the proposed equivalent structure are shown in column (e) of Table 3 with and without the RFID chip model. The real and imaginary parts of the proposed model without the chip show -25% and -2.68% variation and with chip -18% and 22.7% respectively with respect to 3D near body modelling. The results show a close approximation to the CST 3D near body simulation.

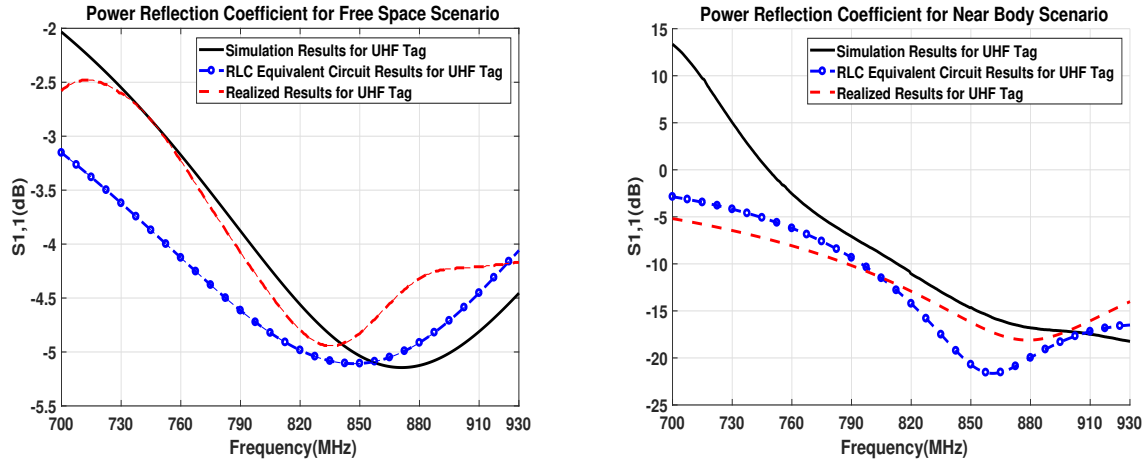

(a) (b)

Fig. 14: Power reflection coefficient for (a) Free space scenario (b) Near body scenario

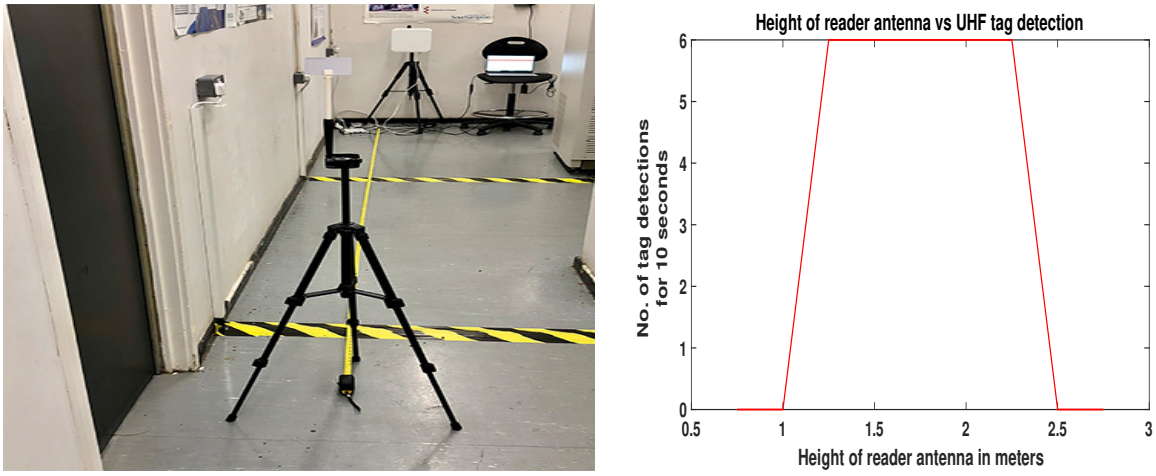

(a) (b)

Fig. 15: Effect of reader antenna variable heights on UHF tag detection. (a) Laboratory testing environment (b) Graphical representation of reader antenna height vs tag detection.

5 FABRICATION AND MEASUREMENT RESULTS ANALYSIS

There are different methods suggested in the literature to test realized antennas. In case of symmetrical geometry, due to the balanced structure of dipole tag antennas, it is not possible to measure them directly because the testing equipment has unbalanced terminated ports. Thus, a balanced antenna, if connected with the unbalanced testing ports will not provide correct impedance response as the current flow to the two radiators of the antenna terminals is not equal. Different methods are proposed to test the RFID tags, such as single ended probes based on unbalanced testing ports which is not suitable for balanced structures. A balun is used for balanced antennas such as dipole antennas, effectively forcing equal current distribution in both radiators of the antenna structure. The Imaging method is used for balanced structures by mounting half part of the antenna on a ground plane which provides the mirror image to replicate the other half structure by doubling the impedance of measured half structure. Differential probes are widely used for measuring balanced antennas based on S parameters and two port network analyzer method [11].

For experimental evaluation, the UHF tag is fabricated on a PET substrate via a screen printing process. The PET substrate has the thickness of 0.05 mm and aluminum etching has 0.01 mm thickness as shown in Fig. 12. The measurement setup is established with a two port Anritsu MS2028C 20 GHz Vector Network Analyzer and a balun with differential probes mounted on an ABS material holder to firmly hold a tag antenna under test. One end of a test fixture consist of two SMA connectors that are connected with VNA and placed outside the anechoic chamber and the other end has extension of two inner conductors of coaxial cable to connect with the ports of an antenna. The length of both coaxial cables is 103 mm. Two port full calibration was performed on VNA to achieve high performance and measurement accuracy, while a port extension technique was applied to eliminate the effect of measurement fixture and to shift the calibration plane from ends of SMA connectors to the tips of fixture where antenna is placed.

A power reflection coefficient graph comparison has been performed between the simulation, RLC equivalent circuit and the realized UHF tag for free space and near body scenarios shown in Fig. 14(a) and Fig. 14(b), respectively. It can be seen from the graphs that the

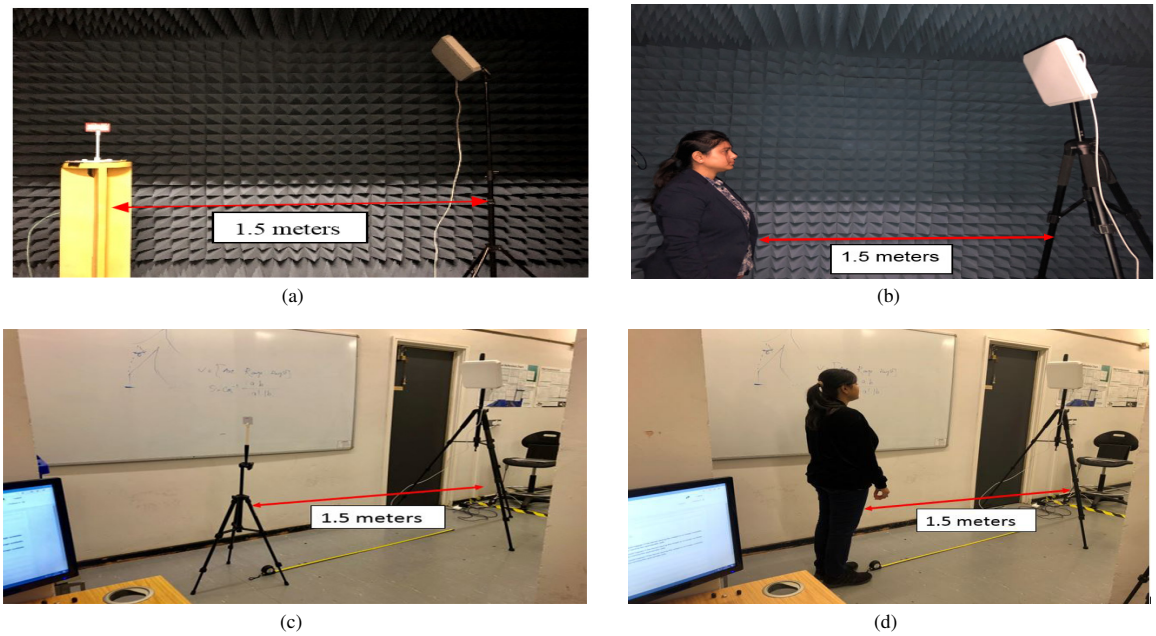

Fig. 16: UHF tag testing environment scenario: (a) Free space in anechoic chamber (b) Near body in anechoic chamber (c) Free space in open air (d) Near body in open air.

power reflection values of both scenarios shows a good comparison with the simulation results using CST. Moreover, the free space scenario shows a lower power reflection value as compared to the near body scenario. The reasons of the high resistance value of 34.25 + j125.37 Ω is due to the high dielectric nature of the human body as shown in Table 3 column (c) at 866 MHz and good impedance matching of the antenna with the RFID chip through design optimisation to perform well near the body.

To facilitate multiple features on a single smart card, a combination of two other tags is also suggested. LF antennas are conventionally used for access control and item level identification, whereas HF antennas can be widely use in smart shelves, library books, contactless payments and asset tracking [29]. The smart card has low frequency and high frequency antennas such as OMT LF antenna and a Circus NXP HF antenna respectively as shown in Fig. 13. Although there are less chances of frequency interaction as these antennas operate at different frequencies, but some mutual coupling effect can be seen if multiple antennas are placed close to each other [30]. To ensure the maximum performance of these three tags at different frequencies, there must be suitable space between each tag boundary. The tags are tested on a smart card with distance varying from 1-7mm to find out the optimum distance required between the boundaries of tags. After several variations, it is verified that there must be at least 5 mm distance among individual tags to ensure that all the tags perform reasonably in the presence of other frequency band tags placed in close proximity.

The height of the reader antenna is considered an important aspect to determine the detection of the card in any environment. An experimental setup has been established at the LSBU laboratory to analyse the impact of reader antenna height on the number of detections as shown in Fig. 15(a). The UHF reader used in testing is an Impinj Speedway R420 which is compatible with EPC Gen2 standard connected with the circularly polarized antenna and a frequency range of 865-870 MHz and gain of 5.5 dBi. It can be seen from Fig. 15(b) that 1 to 2.5 meters height variation the reader antenna is able to detect the card at a constant rate. The height of antenna is chosen as 1.5 meters for further set of experiments.

Measurements on the smart card have been performed in the anechoic chamber environment at LSBU as shown in Fig. 16(a), Fig. 16(b) for free space and near body respectively. The distance between the reader and the card is 1.5 meters. The rotator stand is rotated at 15-degree intervals from 0 - 360 degrees to detect the instances of card detection using the Impinj Multireader software. The power levels range from 15 dBm to 30 dBm with an increment of 1 dBm every 14 seconds. The E-plane is recorded by placing the card vertically and the H-plane of the tag is measured by placing the card horizontally on the turn table and repeating the same process as described above. An ABS (Acrylonitrile Butadiene Styrene) material card holder is fabricated to hold the card and to avoid any material interference factors. The same scenario is setup in open air to realise a realistic environment for free space and near body scenarios as shown in Fig. 16(c) and Fig. 16(d) by repeating the same process as mentioned for the anechoic chamber environment and the data is obtained to compare and validate the results of UHF tag for simulation, anechoic chamber and free space scenario. The radiation pattern is recorded in dBm as shown in Fig. 17(a) . A close agreement can be observed between the measured results in simulation, free space and the anechoic chamber environment, highlighting the validity of results in such scenarios. The theoretical read range of the UHF tag can be calculated from the Friss equation if antenna parameters are known [21] (4).

$$r = \frac{\lambda}{4\pi}\sqrt{\frac{P_T G_T G_R \tau}{P_{th}}} \tag{4}$$

Here, λ is the wavelength, P_T is the power transmitted by the reader, G_T is the gain of the transmitting antenna. The maximum transmitted power of the speedway reader is 31.5 dBm [31], the product of $P_T G_T$ is equivalent to the EIRP, the effective radiated power of the reader, G_R is the gain of the receiving tag antenna, P_{th} is the minimum threshold power to activate the RFID tag chip. Whereas, τ is defined as the power transmission coefficient shown as:

$$\tau = \frac{4R_{\text{chip}}R_{\text{ant}}}{|Z_{\text{chip}} + Z_{\text{ant}}|^2} \qquad 0 \leq \tau \leq 1 \tag{5}$$

$Z_{\text{chip}} = R_{\text{chip}} + jX_{\text{chip}}$ is the impedance of the chip and $Z_{\text{ant}} = R_{\text{ant}} + jX_{\text{ant}}$ is the impedance of the tag antenna. Another practical approach to calculate the maximum read range of RFID tags

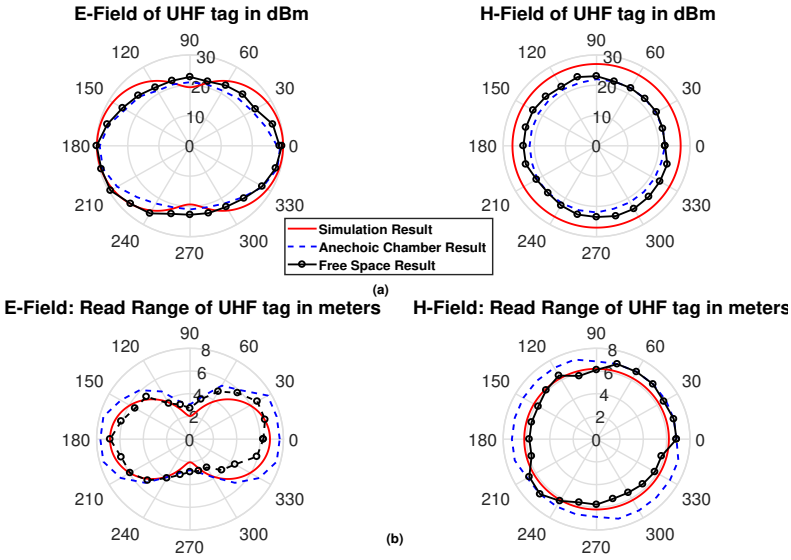

Fig. 17: (a) E-plane and H-plane of UHF tag in free space. (b) Read range of UHF tag in free space.

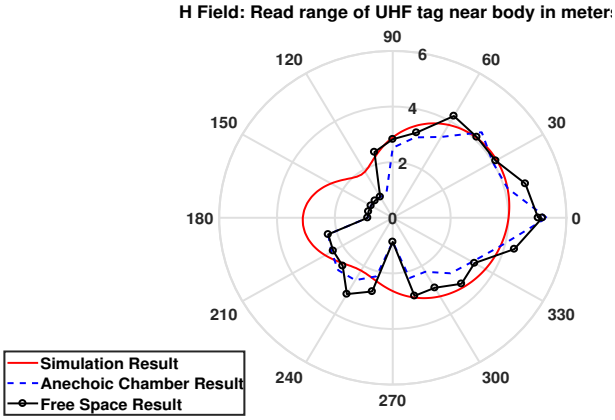

Fig. 18: Read range of UHF tag near the body.

by avoiding simulation errors and practical test mishandling is by modifying the Friss equation and using maximum P_{EIRP} (Effective isotropic Radiated Power) which is 3.3 Watt for the European region and is allocated for RFID applications by government authorities, P_{th} being the minimum threshold power to turn on the RFID chip, G_T being the maximum gain of the transmitting antenna as shown in [26] and [31](6).

$$r = d_{\max}\sqrt{\frac{\mathrm{EIRP}}{P_{th}G_T}} = d_{\max}\sqrt{\frac{\mathrm{EIRP}_{\max}}{\mathrm{EIRP}_{\mathrm{ref}}}} \qquad (6)$$

Now, to calculate the read range of UHF tag at 866 MHz, (4) and (5) are evaluated in MATLAB for the simulation results, (6) is evaluated for the realized results obtained from the anechoic chamber and a comparison is performed as shown in Fig. 17(b). The realized results show the high read range of 7.7 meters and 2.8 meters at the blind spots of E plane and 7.2 meters in the H plane.The obtained results show the appropriateness of UHF tag's performance for long read range especially at the blind spots where the tag antenna is still achieving 2.8 meters read range which is not a common case among the antennas discussed in the literature.

The UHF tag performance is now analysed for near body scenario with a person holding the smart card in the pocket and standing at the same distance of 1.5 meters in an anechoic chamber and in open air as shown in Fig. 16 (c) and (d). The readings are recorded for H-plane of the UHF tag as this is the realistic position of the card in the pocket while the person moves from 0 to 360 degrees at 15-degree increment and the power of reader is level up from 15 dBm to 30 dBm with the increment of 1 dBm. As the smart card aligns vertically with the pocket so the simulations of the YZ plane are compared with the realized scenario and the results obtained are shown in Fig. 18. It can be seen that the maximum read range obtained near the body is 5.2 meters and the minimum read range at the blind spots of the antenna is 2.8 meters, showing the in tag resilience near the body scenario especially at the blind spots, proving it suitable for near body applications.

It can be observed that the read range of UHF tag is consistent in the free space and near body scenario. The geometry of the antenna is highly resilient towards body influence in terms of signal absorption and offers an excellent solution for low or no detection of individuals holding cards near the body. The directivity of the antenna in the near body scenario is higher at the main beam direction (zero degree), it shows energy is well radiated and accepted by antenna, hence the read range is enhanced in this direction. However, the RFID tag becomes unidirectional due to the presence of the human body. Therefore, the human body can be considered an obstacle, creating blind spots in practical scenarios. The proposed tag performance is compared with relevant literature as shown in Table 5 showing it's

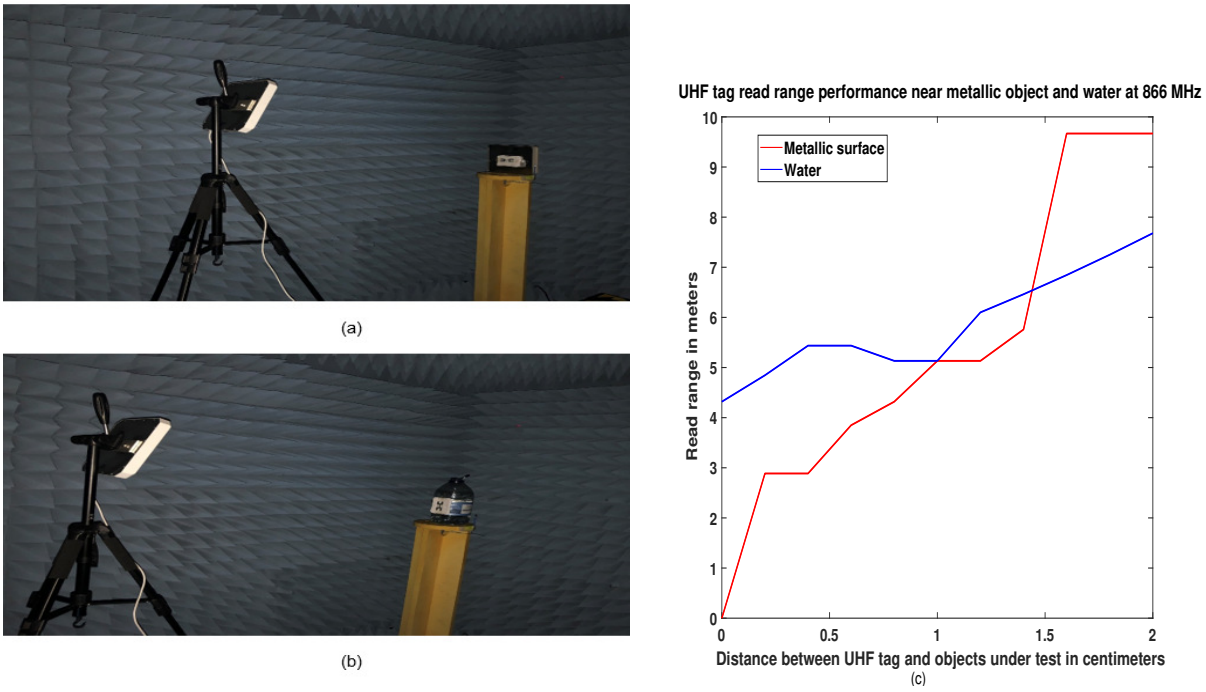

Fig. 19: UHF tag experimental performance analysis in anechoic chamber. (a) Near metal (b) Near bottle of water (c) Graphical representation of read range vs gap between objects and UHF tag antenna.

novelty as compared to other UHF tags in the literature.
Another approach used to validate the uniqueness of tag antenna is by testing the tag in the anechoic chamber in proximity to a metallic surface and on a bottle of water as shown in Fig. 19(a) and Fig. 19(b), respectively, to analyse performance near high dielectric materials that cause a drastic reduction in the read range due to resistance losses. In the literature, several solutions are proposed to overcome this issue such as introducing a sheet of styrofoam or ground plane in the antenna structure but they add considerable size and cost, while the read range improvement is negligible in line of sight measurement [16], [17]. Conversely, the proposed design is capable of performing without any design modification or ground plane insertion. The UHF tag antenna is tested by directly placing on both metal and water bottle surface and by adding paper of variable thickness from 0.2 to 2 cm to investigate the impact on the read range performance. The obtained results are shown in Fig. 19(c), it can be seen that the tag does not respond to the metal but with just 0.2 cm gap it is able to achieve a read range of 2.9 meters and with 2 cm gap it has the read range of 9.6 meters which is very high as compared to existing published work as shown in Table 5. Likewise, the performance of tag antenna near the water bottle offers the read range of 4.3 meters by direct placement on bottle and up to 7.7 meters by introducing a 2 cm gap using paper between the bottle surface and antenna. All the results are compared in Table 5 with existing literature work to show the contribution of proposed UHF tag antenna which is an ideal candidate for free space, near body, metallic surfaces and water.

6 CONCLUSION

This work describes the design, simulation and realization of a small footprint wideband UHF tag antenna with dimensions of $25.14 \times 69.80 \times 0.05$ mm^3 to target smart card limited areas for diverse near body applications. The proposed antenna has a lower volume employing a PET substrate and high read range of up to 5.2 meters for near body applications and 7.7 meters of read range in free space environment. A close approximation of the equivalent RLC circuit for the considered scenarios is provided to initially visualize potential antenna properties. The tag antenna provides read range of nearly 2.8 meters at blind spots, reducing the chances of missed detections. To show the novelty and high resilience, the UHF tag antenna is tested against high dielectric materials such as metallic objects and water and still offers high read range of 2.9 to 9.6 meters and 4.3 to 7.7 meters receptively when a gap is introduced between the tag and objects surface. This proves the tag is indeed suitable for more commonly signal limiting real life scenarios.

7 Acknowledgements

This work has been carried out as part of the Match funded PhD research project in collaboration with London South Bank University and Reward Technology. The authors are grateful to the Reward Technology team for providing support throughout the project.

8 References

1 Chan, H.L., Choi, T.M., Hui, C.L., Ng, S.F.: 'Quick response healthcare apparel supply chains: Value of RFID and coordination', *IEEE Transactions on Systems, Man, and Cybernetics: Systems*, 2015, **45**, (6), pp. 887–900
2 Gu, C.: 'Fast discrepancy identification for RFID-enabled iot networks', *IEEE Access*, 2018, **6**, pp. 6194–6204
3 Zhang, J., Tian, G., Marindra, A., Sunny, A., Zhao, A.: 'A review of passive RFID tag antenna-based sensors and systems for structural health monitoring applications', *Sensors*, 2017, **17**, (2), pp. 265
4 Ziai, M.A., Batchelor, J.C. 'UHF RFID tag antenna design for on-body applications'. In: Antennas and Propagation Conference (LAPC), 2010 Loughborough. (IEEE, 2010. pp. 185–188
5 Dubok, A., Smolders, A.: 'Miniaturization of robust UHF RFID antennas for use on perishable goods and human bodies', *IEEE Antennas and Wireless Propagation Letters*, 2014, **13**, pp. 1321–1324
6 Santiago, A.G., Fernandes, C.A., Costa, J.R. 'Broadband UHF RFID passive tag antenna for near-body operation'. In: RFID-Technologies and Applications (RFID-TA), 2012 IEEE International Conference on. (IEEE, 2012. pp. 271–274

Table 5 Comparison of proposed work with previous literature work.

References	Dimensions	Volume	Gain	Read range in free space	Read range near the body	Read range near metallic object	Read range near water bottle
	mm	mm^3	dB	m	m	m	m
[32]	$20 \times 65 \times 0.5$	650	-16.70	-	1.2	-	-
[5]	$30 \times 120 \times 1.5$	5400	-	-	3	-	2.5
[6]	$67.5 \times 137 \times 1.575$	14565	-	4.2	1.8	1.1	1.1
[33]	50×80	800	-		4.6		
[16]	$70 \times 9.5 \times 0.5$	332.5	-	-	-	2	-
[15]	$58 \times 34 \times 0.8$	1578	-10.11	-	2.2	2	-
[15]	$53 \times 28 \times 0.8$	1188	-9.15	-	2.3	2.2	-
[17]	$80 \times 80 \times 1$	6400	-22.17	2.2	-	-	0.54
[34]	$70 \times 30 \times 3$	6300	-15.1	-	-	-	1.9
Proposed Design	$25.14 \times 69.80 \times 0.05$	87.73	-10.82	7.7	5.2	2.9	4.3

7 Occhiuzzi, C., Calabrese, C., Marrocco, G.: 'Body-matched slot antennas for radiofrequency identification', *XXIX URSI General Assembly*, 2008, pp. 7–16
8 Koski, K., Koski, E., Björninen, T., Babar, A.A., Ukkonen, L., Sydänheimo, L., et al. 'Practical read range evaluation of wearable embroidered UHF RFID tag'. In: Antennas and Propagation Society International Symposium (APSURSI), 2012 IEEE. (IEEE, 2012. pp. 1–2
9 Koskinen, T., Rahmat.Samii, Y. 'Metal-mountable microstrip RFID tag antenna for high impedance microchip'. In: 2009 3rd European Conference on Antennas and Propagation. (IEEE, 2009. pp. 2791–2795
10 Rajagopalan, H., Rahmat.Samii, Y. 'Conformal RFID antenna design suitable for human monitoring and metallic platforms'. In: Proceedings of the Fourth European Conference on Antennas and Propagation. (IEEE, 2010. pp. 1–5
11 Qing, X., Goh, C.K., Chen, Z.N.: 'Impedance characterization of RFID tag antennas and application in tag co-design', *IEEE Transactions on Microwave Theory and Techniques*, 2009, **57**, (5), pp. 1268–1274
12 Tsai, M.C., Chiu, C.W., Wang, H.C., Wu, T.F.: 'Inductively coupled loop antenna design for UHF RFID on-body applications', *Progress In Electromagnetics Research*, 2013, **143**, pp. 315–330
13 Kellomaki, T.: 'On-body performance of a wearable single-layer RFID tag', *IEEE Antennas and Wireless Propagation Letters*, 2012, **11**, pp. 73–76
14 Ukkonen, L., Sydänheimo, L., Rahmat.Samii, Y. 'Sewed textile RFID tag and sensor antennas for on-body use'. In: 2012 6th European Conference on Antennas and Propagation (EUCAP). (IEEE, 2012. pp. 3450–3454
15 Faudzi, N., Rashid, A., Ibrahim, A., Khyasudeen, M., Ali, M. 'Microstrip dipole UHF-RFID tag antenna for metal object tagging'. In: 2016 International Conference on Computer and Communication Engineering (ICCCE). (IEEE, 2016. pp. 36–41
16 Park, C.R., Eom, K.H.: 'RFID label tag design for metallic surface environments', *Sensors*, 2011, **11**, (1), pp. 938–948
17 Sohrab, A.P., Huang, Y., Hussein, M., Kod, M., Carter, P.: 'A UHF RFID tag with improved performance on liquid bottles', *IEEE Antennas and Wireless Propagation Letters*, 2016, **15**, pp. 1673–1676
18 Qin, C., Mo, L., Zhou, H., Zhang, H.: 'Dual-dipole UHF RFID tag antenna with quasi-isotropic patterns based on four-axis reflection symmetry', *International Journal of Antennas and Propagation*, 2013, **2013**
19 Qu, S.W., Ruan, C.L.: 'Effect of round corners on bowtie antennas', *Progress In Electromagnetics Research*, 2006, **57**, pp. 179–195
20 Marrocco, G.: 'The art of UHF RFID antenna design: Impedance-matching and size-reduction techniques', *IEEE antennas and propagation magazine*, 2008, **50**, (1)
21 Riaz, M., Rymar, G., Ghavami, M., Dudley, S. 'A novel design of UHF RFID passive tag antenna targeting smart cards limited area'. In: Consumer Electronics (ICCE), 2018 IEEE International Conference on. (IEEE, 2018. pp. 1–4
22 Santiago, A.G., Costa, J.R., Fernandes, C.A.: 'Broadband UHF RFID passive tag antenna for near-body applications', *IEEE Antennas and Wireless Propagation Letters*, 2013, **12**, pp. 136–139
23 Tribe, J., Oyeka, D., Batchelor, J., Kaur, N., Segura.Velandia, D., West, A., et al. 'Tattoo antenna temporary transfers operating on-skin (tattoos)'. In: International Conference of Design, User Experience, and Usability. (Springer, 2015. pp. 685–695
24 Marrocco, G.: 'RFID antennas for the UHF remote monitoring of human subjects', *IEEE Transactions on Antennas and Propagation*, 2007, **55**, (6), pp. 1862–1870
25 Oyeka, D.O., Batchelor, J.C., Ziai, A.M.: 'Effect of skin dielectric properties on the read range of epidermal ultra-high frequency radio-frequency identification tags', *Healthcare technology letters*, 2017, **4**, (2), pp. 78
26 Sohrab, A.P., Huang, Y., Hussein, M.N., Carter, P.: 'A hybrid UHF RFID tag robust to host material', *IEEE Journal of Radio Frequency Identification*, 2017, **1**, (2), pp. 163–169
27 Zamora, G., Zuffanelli, S., Paredes, F., Mart, F., Bonache, J., et al.: 'Design and synthesis methodology for UHF-RFID tags based on the t-match network', *IEEE Transactions on Microwave Theory and Techniques*, 2013, **61**, (12), pp. 4090–4098
28 Chinen, K., Kinjo, I., Zamami, A., Irei, K., Nagayama, K.: 'New equivalent-electrical circuit model and a practical measurement method for human body impedance', *Bio-medical materials and engineering*, 2015, **26**, (s1), pp. S779–S786
29 Zuffanelli, S.: 'Antenna Design Solutions for RFID Tags Based on Metamaterial-Inspired Resonators and Other Resonant Structures'. (Springer, 2017)
30 Owen, G.J., Braaten, B.D., Nelson, R.M., Vaselaar, D., Bauer.Reich, C., Glower, J., et al. 'On the effect of mutual coupling on lf and uhf tags implemented in dual frequency rfid applications'. In: 2009 IEEE Antennas and Propagation Society International Symposium. (IEEE, 2009. pp. 1–4
31 Deleruyelle, T., Pannier, P., Egels, M., Bergeret, E.: 'An RFID tag antenna tolerant to mounting on materials', *IEEE Antennas and Propagation Magazine*, 2010, **52**, (4), pp. 14–19
32 Ziai, M.A., Batchelor, J.C., et al.: 'Temporary on-skin passive UHF RFID transfer tag', *IEEE Transactions on Antennas and Propagation*, 2011, **59**, (10), pp. 3565–3571
33 Marques, D., Egels, M., Pannier, P.: 'Broadband UHF RFID tag antenna for bio-monitoring', *Progress In Electromagnetics Research*, 2016, **67**, pp. 31–44
34 Liu, Q., Li, H., Yu, Y.F.: 'A versatile flexible UHF RFID tag for glass bottle labelling in self-service stores', *IEEE Access*, 2018, **6**, pp. 59065–59073